Novel unimorph deformable mirror for ocular adaptive optics

Jianqiang Ma, Kai Chen, Junjie Chen, Jiaru Chu

Jianqiang Ma, Kai Chen, Junjie Chen, Jiaru Chu, "Novel unimorph deformable mirror for ocular adaptive optics," Proc. SPIE 9298, International Symposium on Optoelectronic Technology and Application 2014: Imaging Spectroscopy; and Telescopes and Large Optics, 92981E (18 November 2014); doi: 10.1117/12.2071455

SPIE.

Event: International Symposium on Optoelectronic Technology and Application 2014, 2014, Beijing, China

Novel unimorph deformable mirror for ocular adaptive optics

Jianqiang Ma*[a], Kai Chen[a], Junjie Chen[b], Jiaru Chu[b]
[a]Faculty of Mechanical Engineering & Mechanics, Ningbo University, Ningbo 315211, China;
[b]Department of Precision Machinery & Precision Instrumentation, University of Science and Technology of China, Hefei 230027, China;

ABSTRACT

This paper proposes a low-cost unimorph deformable mirror (DM) driven by positive voltages for ocular adaptive optics (AO). The DM consists of an inner actuators array and an outer ring actuator. The inner actuators array is used to correct aberrations, while the outer ring actuator is used to generate an overall defocus bias. The measurement results show that the maximum peak to valley defocus deformation is more than 14 μm. The DM has a satisfactory correction capability for up to the fifth order Zernike mode aberrations. Furthermore, a sample of 200 ocular wavefronts was simulated using a statistical model developed by Thibos. After correction with the developed DM, most of the simulated eyes achieved the diffraction-limited performance. These experimental and simulation results indicate that this DM is satisfactory for ocular applications.

Key words: deformable mirror, model eye, vision science, adaptive optics

1. INTRODUCTION

The human eye is a complex optical system suffered by aberrations. Besides the well known aberrations named as defocus and astigmatism, there are still some other higher order aberrations. The aberrations limit the ability for high resolution of in-vivo imaging of the retina. To solve this, adaptive optics (AO) has been adopted to actively correct those aberrations in real time. The quality of retinal images has been improved greatly in several different retinal imaging instruments, such as scanning laser ophthalmoscope (SLO) [1] and optical coherence tomography (OCT) [2].

Deformable mirror (DM), as a key component of AO system, determinates the correction capability in a sense. Many kinds of commercially available DMs have been successfully used in ocular AO. Each DM has its own advantages and limitations. Devaney [3] compared the performance of eight commercial DMs for ocular AO. It's found that a high Strehl ratio can be obtained in the ocular application with a relatively low number of actuators if the stroke is sufficient. Doble [4] proposed the requirement of an ideal DM which should has a 10 mm diameter, 100 actuators, a 10 μm stroke and 100 Hz bandwidth.

Among various DMs, unimorph or bimorph DMs are attractive due to their low-cost and large stroke (>10 μm) for correcting low-order optical aberrations [5]. In this paper, a new unimorph DM driven by positive voltages is proposed. Also, the ability of the DM for fitting the ocular wavefronts is simulated.

2. DEFORMABLE MIRROR

The layout of the proposed unimorph DM is illustrated in Figure 1. The DM comprises of a 100 μm thick PZT layer and a 200 μm thick silicon layer. These two layers are glued together with edge supported rigidly. The uniform metallization between the silicon layer and the PZT layer is used as the ground electrode. The backside metallization is patterned to form an inner actuator array with 37 hexagonal actuators and an outer ring actuator. The overall size of the DM is 40 mm in diameter, with only the central 15 mm area used for aberration correction.

Due to the restriction of the fixed supported boundary, when the DM is driven by positive voltages, the outer ring actuator generates overall concave defocus; while each inner actuator generates a local convex deflection. These two opposite deformations are counteracted, resulting in a flat surface in the active aperture. The proposed DM is driven by only

* Email: majianqiang@nbu.edu.cn

Intl. Symposium on Optoelectronic Technology and Application 2014: Imaging Spectroscopy; and Telescopes and Large Optics, edited by J. P. Rolland, C. Yan, D. W. Kim, W. Ma, L. Zheng, Proc. of SPIE Vol. 9298, 92981E · © 2014 SPIE · CCC code: 0277-786X/14/$18 · doi: 10.1117/12.2071455

positive voltages that can avoid depolarization and reverse polarization of the thin PZT layer. The DM works as follows: the ring electrode is normally biased at a constant voltage to produce a pre-deformed concave shape that is approximately equal to the half of the maximum convex defocus generated by those 37 inner actuators; while 37 inner actuators are used to correct both positive and negative curvature wavefront aberrations.

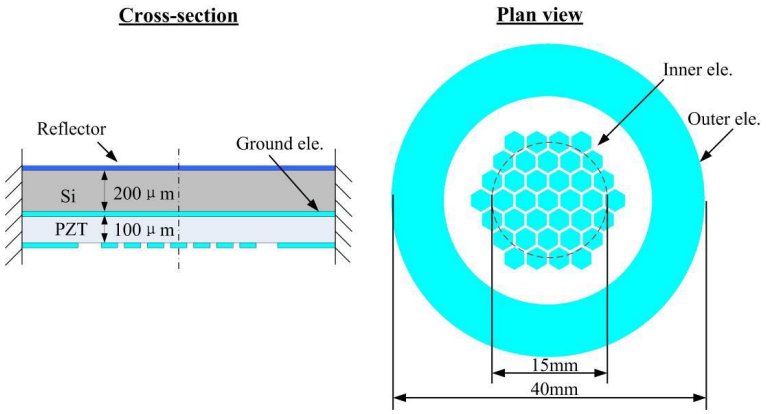

Figure 1. Layout of the unimorph DM driven by positive voltages.

Figure 2. Photograph of the assembled unimorph DM.

The assembled unimorph DM is shown in Figure 2. The DM was fabricated using a simple fabrication process without polish process, described in detail elsewhere [6]. Figure 3 shows the measured deflection of the DM actuators. The stroke of the individual inner actuator is about 5 μm at 100 V. The DM has a maximum peak to valley defocus deformation of -14.3 μm at 150 V for the ring actuator and 14.9 μm at 100 V for the inner actuators array. It is known that wavefront is twice of the mirror deflection, which means that this DM has a potential to compensate large wavefront aberrations.

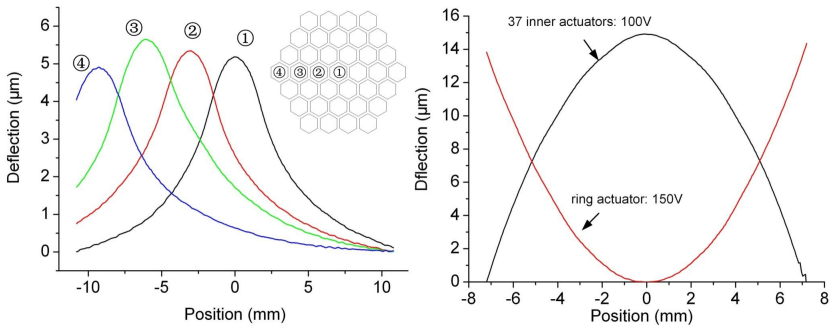

Figure 3. Actuator deflection of the DM. (Left) local deflection of typical inner actuator at 100 V, (Right) whole deflection of inner array and ring actuator.

3. ANALYSIS METHOD

3.1 Close loop control method

Zernike polynomials provide very convenient and quite efficient representation of distorted optical wavefronts of various origins inside circular aperture. The circular mirror surface $\phi(x, y)$ can be expressed as

$$\phi(x,y) = \sum_{k=1}^{m} a_k Z_k(x,y) \tag{1}$$

where m is the total number of Zernike polynomials, and $Z_k(x, y)$ is the kth Zernike mode with a coefficient a_k. A column vector $A = [a_1, a_2, \ldots a_m]^T$ can be used to represent mirror surface $\phi(x, y)$.

The influence function matrix B describes the relationship between the applied control voltages V and the responding mirror deformation A, which is given by

$$A = BV \tag{2}$$

In order to avoid the overlarge voltage calculated using the least-square method, a close-loop control method based on the standard steepest descent algorithm was used. The key iterative formula is expressed as [7]

$$V_{(n)} = V_{(n-1)} - 2\mu B^T (A_{(n-1)} - A_{\text{target}}) \tag{3}$$

where μ is a positive scalar representing the convergence rate. A smaller μ enables better but slower convergence. When all the control voltages V are updated in one step by use of Eq. 3, the total output wavefront error moves toward its minimum.

3.2 Fitting Zernike modes

The correction performance of the DM was eliminated by fitting Zernike modes aberrations using the experimental influence function matrix. The voltage range is from 0 V to 100 V (equivalently to from -50 V to 50 V). The residual wavefront error is the difference between an ideal shape and a simulation shape. The normalized residual wavefront error is defined as the RMS ratio of the residual wavefront error to the ideal shape. The root mean square (RMS) value of wavefront was used for characterization, calculated by

$$\sigma = \sqrt{\sum_{k=1}^{m} a_k^{\,2}} \tag{4}$$

The RMS wavefront and normalized residual wavefront error for each generated Zernike mode shape were calculated and shown in Figure 4. The normalized RMS residual wavefront errors increase with the Zernike modes. The values are less than 0.1 μm before the 15th mode. The DM nearly has no effect for 31st, 32nd, and 33rd modes due to the insufficient of actuators. As expected for a unimorph DM, the DM has a large deformation for low-order Zernike mode aberrations. The RMS value of astigmatism is larger than 2 μm, especially the RMS value of defocus is larger than 4.5 μm. These two aberrations are dominant in ocular AO.

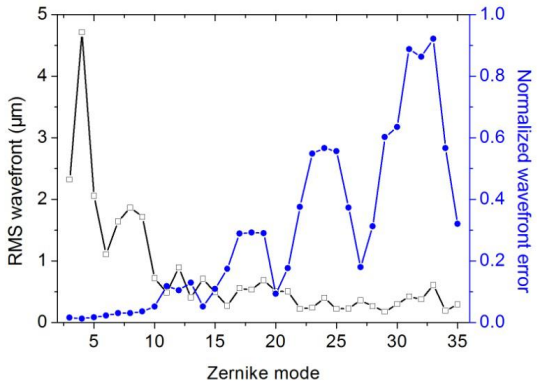

Figure 4. Maximum RMS wavefront and normalized wavefront error of generated Zernike mode shapes.

Furthermore, the Zernike mode shapes up to the fifth order were generated experimentally. The interferograms were shown in Figure 5. The generated shapes fit the theoretical shapes quite well.

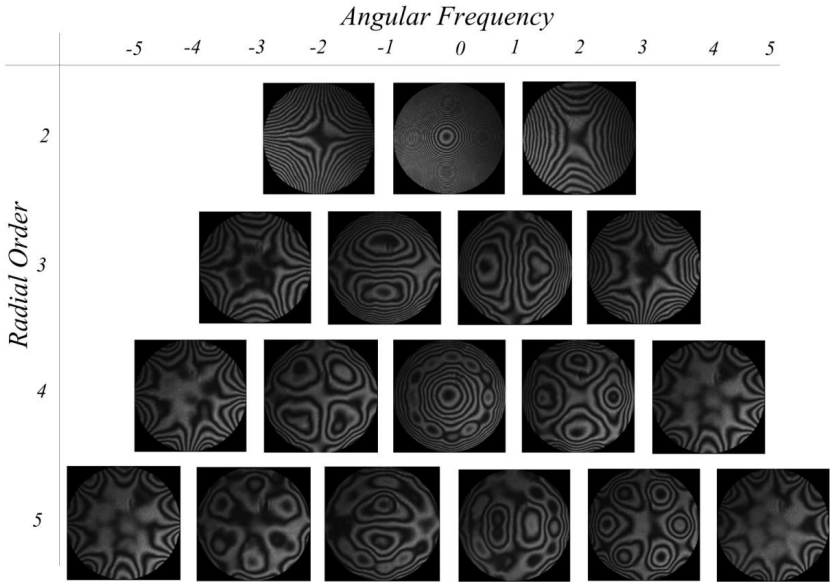

Figure 5. Interferograms of reproduced Zernike mode shapes from 2nd to 5th order.

4. OCULAR ABERRATIONS CORRECTION

4.1 Ocular aberration simulation

The most widely used statistics are those published by Thibos et al. based on a study of the 200 normal, well-corrected eyes [8]. The eyes were corrected subjectively for defocus and astigmatism to the nearest 0.25 diopters (D). The vector of Zernike aberration coefficients describing the aberration function for any individual eye was modelled as a multivariate, Gaussian, random variable with known mean, variance and covariance. We generated 200 typical ocular wavefronts for a 6mm diameter pupil. The ocular wavefronts were decomposed using 36 Zernike polynomials. Piston, tip, and tilt were removed from the Zernike decomposition, since these are usually ignored or precorrected in ocular AO systems.

4.2 Ocular wavefronts aberrations correction

The correction of ocular wavefront aberrations were simulated using Eq. 3. The correction result for one ocular aberration is shown in Figure 6. The RMS wavefront aberration was reduced from 0.697 μm to 0.048 μm. The aberrations before 15th modes have been correct completely, which agree with the correction capability analysis in section 3.2. The residual wavefront error can be further reduced by increasing the actuator number.

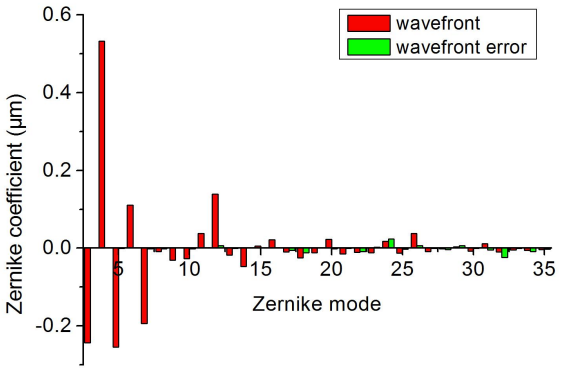

Figure 6. Zernike coefficients of one eye before and after correction.

The correction results for 200 ocular wavefronts are shown in Figure 7. All of these aberrations were eliminated significantly. The mean RMS value of ocular wavefront is 0.671 μm with a standard deviation of 0.258 μm, which was decreased to 0.037 μm with a standard deviation of 0.010 μm. The Strehl Ratio can be calculated by

$$SR = e^{-(\frac{2\pi\sigma}{\lambda})^2} \tag{5}$$

where λ is the wavelength. The corresponding average Strehl ratio is 0.85 for a wavelength of 600 nm, indicating that this DM can achieve diffraction-limited performance (Strehl ratio over 0.8). These results are similar to the results of a 35-channel bimorph DM from AOptix studied by Devaney [3]. Additionally, the maximum voltages needed for correcting ocular wavefront were calculated. Figure 8 shows that the DM still has a margin that is useful in practical applications since the simulated eyes are well-corrected.

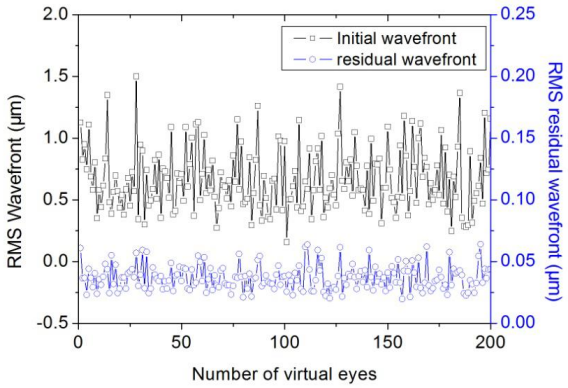

Figure 7. RMS wavefront before and after correction by the fabricated DM. (Piston, tip and tilt terms were removed)

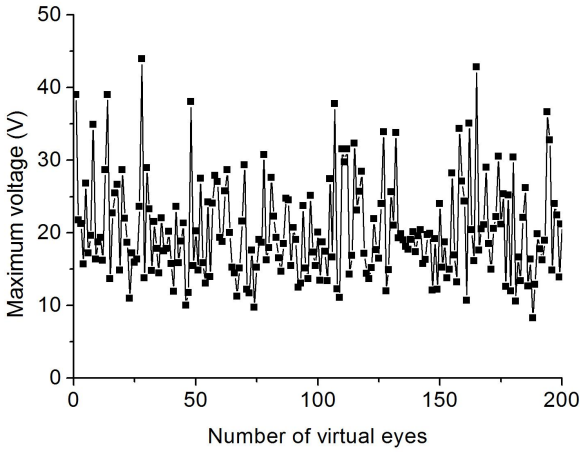

Figure 8. Maximum voltages required for correction.

5. CONCLUSIONS

This paper reported a novel low-cost thin unimorph deformable mirror for ocular adaptive optics. The correction performance of the DM for typical ocular wavefronts was investigated using the close-loop method. 200 ocular wavefronts for a 6mm diameter pupil were generated using eyes model published by Thibos et al. After correction, most of the simulated eyes achieved the diffraction-limited performance. The mean RMS residual ocular wavefront is 0.037 μm with a standard deviation of 0.010 μm. From the simulation results, the actuators of the DM should be further increased to further improve the correction capability.

6. ACKNOWLEDGMENTS

This work was supported by National Natural Science Foundation of China (11303019), Zhejiang Provincial Natural Science Foundation of China (LQ13E050016), Ningbo Natural Science Foundation (2013A610047), Project of Education Department of Zhejiang Province (Y201326728) and the scientific research fund of Ningbo University (xkl1325).

REFERENCES

[1] Roorda, A., Romero-Borja, F., Donnelly, W. J., Queener, H., Hebert, T. J., and Campbell, M. C. W., "Adaptive optics scanning laser ophthalmoscopy," OPTICS EXPRESS, 10(9), 405-412 (2002).

[2] Zawadzki, R. J., Choi, S. S., Fuller, A. R., Evans, J. W., Hamann, B., and Werner, J. S., "Cellular resolution volumetric in vivo retinal imaging with adaptive optics-optical coherence tomography," OPTICS EXPRESS, 17(5), 4084-4094 (2009).

[3] Devaney, N., Dalimier, E., Farrell, T., Coburn, D., Mackey, R., Mackey, D., Laurent, F., Daly, E., and Dainty, C., "Correction of ocular and atmospheric wavefronts: a comparison of the performance of various deformable mirrors," Applied Optics, 47(35), 6550-6562 (2008).

[4] Doble, N., and Williams, D. R., "The application of MEMS technology for adaptive optics in vision science," Ieee Journal of Selected Topics in Quantum Electronics, 10(3), 629-635 (2004).

[5] Horsley, D. A., Park, H., Laut, S. P., and Werner, J. S., "Characterization of a bimorph deformable mirror using stroboscopic phase-shifting interferometry," Sensors and Actuators a-Physical, 134(1), 221-230 (2007).

[6] Ma, J., Liu, Y., He, T., Li, B., and Chu, J., "Double Drive Modes Unimorph Deformable Mirror for Low-Cost Adaptive Optics," Applied Optics, 50(29), 5647-5654 (2011).

[7] Zhu, L. J., Sun, P. C., Bartsch, D. U., Freeman, W. R., and Fainman, Y., "Adaptive control of a micromachined continuous-membrane deformable mirror for aberration compensation," Applied Optics, 38(1), 168-176 (1999).

[8] Thibos, L. N., "Retinal image quality for virtual eyes generated by a statistical model of ocular wavefront aberrations," Ophthalmic and Physiological Optics, 29(3), 288-291 (2009).